PLASTIC DEFORMATION OF BEAMS IN STEEL MOMENT-RESISTANT FRAMES SUBJECTED TO STRONG EARTHQUAKES

NAKAHARA Hiroaki[1], YAMANARI Minoru[2] and OGAWA Koji[2]

[1]Graduate School of Science and Technology, Kumamoto University
[2]Department of Architecture, Faculty of Engineering, Kumamoto University
2-39-1 Kurokami, Kumamoto 860-8555 Japan

ABSTRACT

This study is concerned with the demand for ductility of beams in steel moment-resistant frames. Numerical response analysis was carried out for 15 frames against a variety of ground motions. This paper describes the magnitude of plastic deformation introduced into beam-ends. The purpose of this study is to deduce the demand for ductility of beams. Maximum plastic rotation, maximum increment of plastic rotation during a half-cycle of vibration, and the range of variable plastic rotation are considered as the parameters that represent the magnitude of plastic deformation. The results are summarized as formulas to predict those parameters based on maximum story drift angles.

KEYWORDS

Beams, steel moment-resistant frames, earthquake response, maximum plastic rotation, maximum story drift angles, ductility demand, performance-based design

1. INTRODUCTION

The Hyogoken-Nanbu (Kobe) earthquake (1995) caused serious damage to modern steel building structures. Among various types of damage observed, fractures at welded beam-to-column connections in moment-resistant frames posed one of the most serious concerns for the structural engineering community. This had led to urgent research efforts on quantification of (plastic) rotations demanded of beam-ends and beam-to-column connections when steel moment frames are subjected to large earthquakes. Performance-based design has also been explored extensively since those earthquakes. Therefore, it is considered that specifying maximum story drift angles as a desired value of the design at first stage of the design will be common in the future.

It is obvious that various structural properties such as building height, strength and stiffness distributions along the height, column-to-beam relative strength, also significantly affect earthquake responses (maximum story drifts and beam rotations of steel moment frames). However, if the relationship between maximum story drift angles and the plastic deformation introduced into beam-ends can be clarified, the demand for ductility of beams can be known at the stage that maximum story drift angles was specified. Then, in this

TABLE 1. Analyzed frames.

Name	Story number	Beam-to-column strength ratio	Ultimate base shear coefficient	First natural period
AR02	2	2.202 ∼ 2.202	0.572	0.606
AR04	4	2.054 ∼ 2.310	0.425	0.820
AR08	8	1.812 ∼ 2.592	0.405	1.173
AR12	12	1.938 ∼ 3.015	0.284	1.625
BR02	2	1.275 ∼ 1.275	0.813	0.541
BR04	4	1.329 ∼ 1.405	0.526	0.800
BR08	8	1.513 ∼ 1.906	0.492	1.148
BR12	12	1.564 ∼ 2.219	0.345	1.576
CR02	2	2.070 ∼ 2.070	0.501	0.629
CR04	4	1.928 ∼ 2.648	0.404	0.841
CR08	8	1.480 ∼ 3.051	0.365	1.159
BRI3A	3	2.897 ∼ 3.032	0.557	0.638
BRI3B	3	2.367 ∼ 2.398	0.506	0.688
BRI9A	9	1.789 ∼ 2.976	0.209	1.882
BRI9B	9	1.722 ∼ 2.384	0.227	1.834

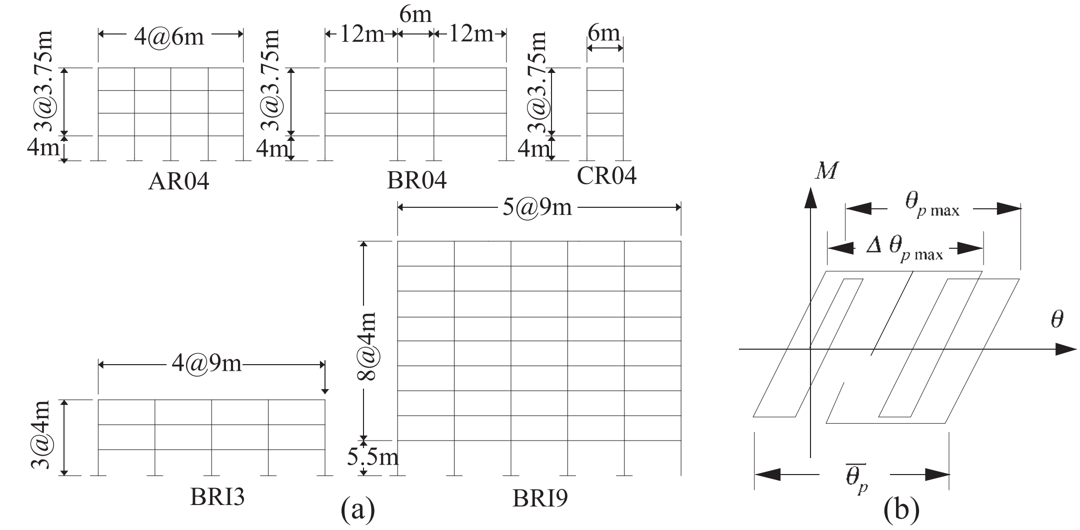

Figure 1: Outline of analysis: (a) Shapes of the frames, (b) Parameters.

study, based on the result of earthquake response analysis for row-and-middle rise standard steel moment-resistant frames, the authors determined the relationship between maximum story drift angles and the plastic deformation introduced into beam-ends.

2. OUTLINE OF ANALYSIS

Analyzed frames are shown in TABLE 1. All frames are steel moment-resistant frames consisting of rectangular hollow section steel columns and wide-flange steel beams. The shapes of the frames are shown in Figure 1(a). There are two-, eight-, and twelve-story frames in AR and BR besides four-story frame shown in figure 1(a). These frames are the same in the number of spans and span length. There are two-, and eight-story frames in CR besides four-story frame shown in figure 1(a). These frames are also the same in the number of spans and span length. There are two kinds of frames, A and B, in BRI3 and BRI9. These frames are the same in the number of story, story height, in the number of spans, and span length, respectively, but different a designer.

Suites of ground motions used in the FEMA/SAC project (3) were used for the dynamic response analysis of the frames. They were the two sets of 20 records that represent probabilities of excess of 10 and 2 per cent in 50 years in the U.S. Los Angeles area, denoted as the 10/50 and 2/50 record sets.

A program code developed by the third author Ogawa was used for the analysis. In this study, three values shown in Figure 1(b) were chosen as the parameters that represent the magnitude of plastic deformation of beams. That is, maximum plastic rotation ($\theta_{p\,\max}$), maximum increment of plastic rotation during a half-cycle of vibration ($\Delta\,\theta_{p\,\max}$), and the range of variable plastic rotation ($\overline{\theta_p}$). However, in this study, maximum plastic rotation ($\theta_{p\,\max}$) is considered to be the most important parameter, and responses are arranged about beam-ends occurred the largest maximum plastic rotation among beam-ends in each story in each analysis.

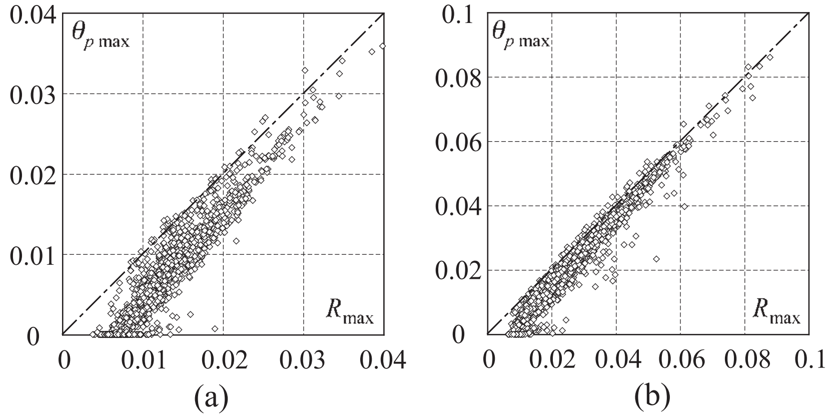

Figure 2: Relationship between $R_{\max}$ and $\theta_{p\,\max}$: (a) 10/50; (b) 2/50.

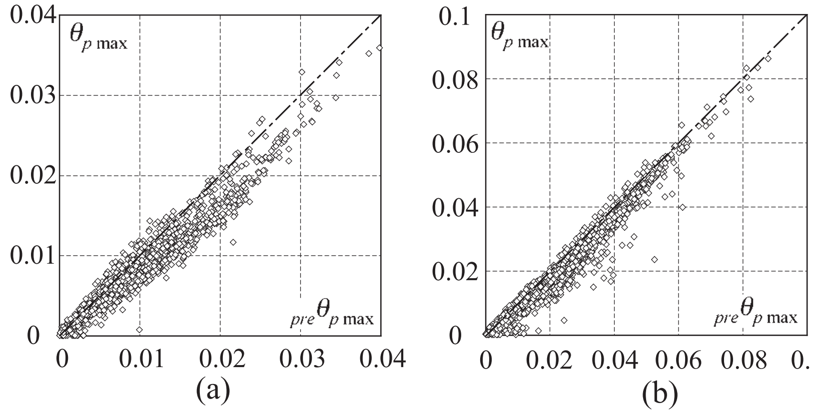

Figure 3: Relationship between ${}_{pre}\theta_{p\,\max}$ and $\theta_{p\,\max}$: (a) 10/50, (b) 2/50.

3. RELATIONSHIP BETWEEN $R_{\max}$ AND $\theta_{p\,\max}$

3.1 Maximum plastic rotation $\theta_{p\,\max}$

The relationship between a mean value of maximum story drift angles above and below each floor level ($R_{\max}$) and maximum plastic rotation ($\theta_{p\,\max}$) is shown in Figure 2. According to Figure 2, $R_{\max}$ is almost upper limit of $\theta_{p\,\max}$. Especially, in large deformation region, it is recognized that $R_{\max}$ tends to become good approximate values of $\theta_{p\,\max}$. On the other hand, in the range that $R_{\max}$ is less than about 0.02, $\theta_{p\,\max}$ is very scattered and although $R_{\max}$ tends to become upper limit of $\theta_{p\,\max}$, $R_{\max}$ cannot become the approximate values of $\theta_{p\,\max}$. On the basis of a method proposed in a Reference (1), in the range that $R_{\max}$ is comparatively small, ${}_{pre}\theta_{p\,\max}$ (approximate values of $\theta_{p\,\max}$) should be expressed by using $R_{\max}$.

$$ {}_{pre}\theta_{p\,\max} = \frac{3}{2}\,(\,R_{\max} - R_y\,) \tag{1} $$

In which R_y is the story drift angles when plastic hinges are first formed at beam-ends under an earthquake. Eqn.1 is introduced by the assumption that deformations progress in a state that plastic hinges are formed at only one end of beams. If the deformations become large and plastic hinges are formed at both ends of beams, although Eqn.1 cannot be used, $\theta_{p\,\max}$ is able to be approximated by $R_{\max}$ in the range that $R_{\max}$ is large as shown in Figure 2. The approximate values of the largest maximum plastic rotation in each story (${}_{pre}\theta_{p\,\max}$) are able to be expressed.

$$ {}_{pre}\theta_{p\,\max} = \min\,\{\frac{3}{2}\,(\,R_{\max} - R_y)\,,\, R_{\max}\} \tag{2} $$

The relationship between the approximate values (${}_{pre}\theta_{p\,\max}$) and responses ($\theta_{p\,\max}$) is shown in Figure 3. According to Figure 3, the relationship between the approximate values of Eqn.2 (${}_{pre}\theta_{p\,\max}$) and responses ($\theta_{p\,\max}$) is settled in the narrow band. In addition, although not shown in Figure 2, 3, the largest values in each story of analysis results ($\theta_{p\,\max}$) were almost occurred by negative bending that upper flanges are

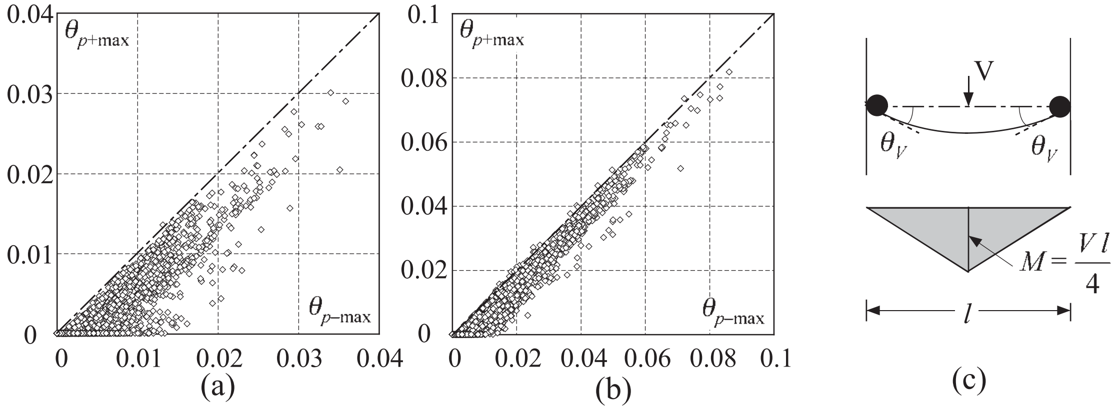

Figure 4: (a) 10/50 ($\theta_{p-\max}$ and $\theta_{p+\max}$), (b) 2/50 ($\theta_{p-\max}$ and $\theta_{p+\max}$), (c) Plastic rotation.

subjected to tension force. The case that plastic rotation of positive bending that bottom flanges are subjected to tension force was greater than plastic rotation of negative bending was only 20 analysis results among 3600 all analysis results. As the cause that plastic rotation of negative bending was greater than plastic rotation of positive bending, effects of bending moment occurred by static vertical load are considered.

3.2 Maximum story drift angles of positive bending

Most of maximum plastic rotation ($\theta_{p\,\max}$) examined for the foregoing paragraph is the maximum plastic rotation of negative bending ($\theta_{p-\max}$).

$$\theta_{p\,\max} \simeq \theta_{p-\max} \tag{3}$$

On the other hand, many of brittle fractures at beam-ends observed in the Hyogoken-Nanbu (Kobe) earthquake were occurred at the bottom flanges, which are considered by positive bending. Here the relationship between the largest values in each story of plastic rotation of the negative bending ($\theta_{p-\max}$) and the largest values in each story of plastic rotation of positive bending ($\theta_{p+\max}$) is examined. However, although the reasons that the brittle fractures at beam-ends tend to occur at the bottom flanges are effects of floor slabs, in this analysis, effects of floor slabs on beam stiffness and strength are neglected. The relationship between $\theta_{p-\max}$ and $\theta_{p+\max}$ in each story in all analysis results is summarized in Figure 4(a), (b). Although it is obvious that $\theta_{p-\max}$ tends to become larger than $\theta_{p+\max}$ as shown in Figure 4(a), (b), even if $\theta_{p+\max}$ becomes large, it is not recognized that the difference of $\theta_{p-\max}$ and $\theta_{p+\max}$ extends.
If plastic deformations occurred at both ends of beams under concentrated loading are assumed to correspond to the rotation of a simple beam (θ_V) as shown in Figure 4(c). Namely,

$$\theta_V = \frac{V\,l^2}{16\,E\,I} \tag{4}$$

In which V is a static vertical load; l is the length of a simple beam; E is Young's modulus; I is the moment of inertia. After plastic hinges rotated as shown in Figure 4(c), the influence that the vertical load affects plastic rotation increment is canceled and even if the frames deformed into any direction, it is expected that the plastic hinges of both ends are occurred the same plastic rotation increment of a positive-negative opposite direction. Therefore, it can be deemed that the difference of $\theta_{p-\max}$ and $\theta_{p+\max}$ can be approximated by $2\,\theta_V$ if the state occurred this plastic rotation of negative bending (θ_V) is assumed to be a neutral state of vibration. Namely,

$$\theta_{p-\max} - \theta_{p+\max} \simeq 2\,\theta_V \tag{5}$$

The relationship between ($\theta_{p-\max} - \theta_{p+\max}$) and $2\,\theta_V$ is shown in Figure 5. In the range that $\theta_{p-\max}$ is smaller than 0.01, ($\theta_{p-\max} - \theta_{p+\max}$) varies in the range from $2\,\theta_V$ or 0.01 to zero. On the other hand, in the range that $\theta_{p-\max}$ is larger than 0.01, ($\theta_{p-\max} - \theta_{p+\max}$) becomes the values near $2\,\theta_V$, and if $\theta_{p-\max}$ more than about 0.01 is considered, Eqn.5 are generally materialized.

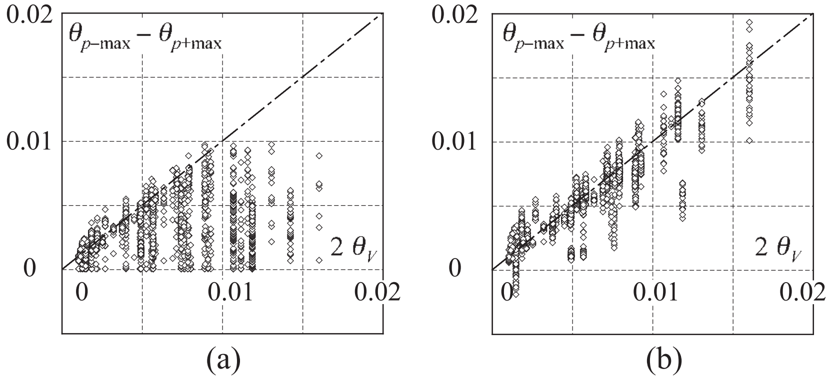

Figure 5: Relationship between ($\theta_{p-\max} - \theta_{p+\max}$) and $2\,\theta_V$: (a) $\theta_{p-\max} < 0.01$, (b) $0.01 < \theta_{p-\max}$.

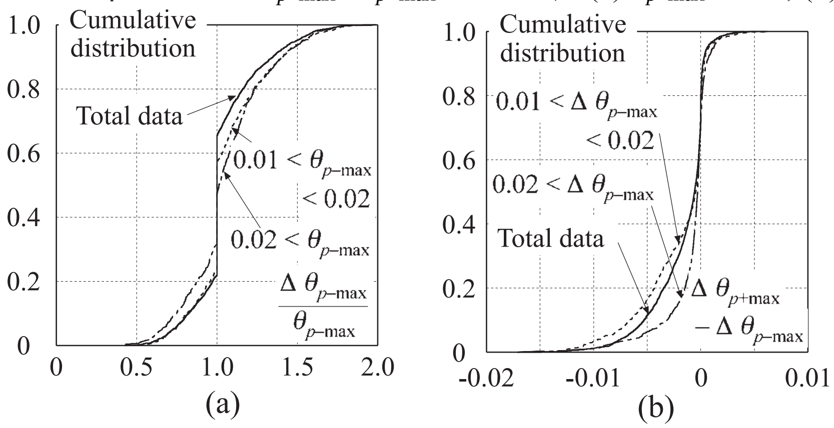

Figure 6: Cumulative distribution: (a) $\Delta\,\theta_{p-\max} / \theta_{p-\max}$, (b) $\Delta\,\theta_{p+\max} - \Delta\theta_{p-\max}$.

3.3 Maximum plastic rotation increment $\Delta\,\theta_{p\,\max}$

It is defined that maximum increment of plastic rotation during a half-cycle of vibration at beam-ends occurred $\theta_{p-\max}$ is $\Delta\,\theta_{p-\max}$, and maximum increment of plastic rotation during a half-cycle of vibration at beam-ends occurred $\theta_{p+\max}$ is $\Delta\,\theta_{p+\max}$. Cumulative distribution of the ratio of $\Delta\,\theta_{p-\max}$ and $\theta_{p-\max}$ is shown in Figure 6(a). According to Figure 6(a), regardless whether the size of $\theta_{p-\max}$, the ratio of $\Delta\,\theta_{p-\max}$ and $\theta_{p-\max}$ is concentrated near 1, and $\Delta\,\theta_{p-\max}$ can be approximated by $\theta_{p-\max}$. Namely,

$$\Delta\,\theta_{p-\max} \simeq \theta_{p-\max} \tag{6}$$

Cumulative distribution of the difference of $\Delta\,\theta_{p+\max}$ and $\Delta\,\theta_{p-\max}$ is shown in Figure 6(b). Although it is recognized that $\Delta\,\theta_{p-\max}$ tends to become a little larger than $\Delta\,\theta_{p+\max}$ in the small range of $\Delta\,\theta_{p-\max}$, anyway the difference of $\Delta\,\theta_{p+\max}$ and $\Delta\,\theta_{p-\max}$ is concentrated near zero.

$$\Delta\,\theta_{p-\max} \simeq \Delta\,\theta_{p+\max} \tag{7}$$

3.4 The range of variable plastic rotation $\overline{\theta_p}$

It is defined that the range of variable plastic rotation at beam-ends occurred $\theta_{p-\max}$ is $\overline{\theta_{p-}}$, and the range of variable plastic rotation at beam-ends occurred $\theta_{p+\max}$ is $\overline{\theta_{p+}}$. Cumulative distribution of the difference of $\overline{\theta_{p-}}$ and $\overline{\theta_{p+}}$ is shown in Figure 7(a) by dividing into the size of $\overline{\theta_{p-}}$. According to Figure 7(a), as $\overline{\theta_{p-}}$ becomes large, the difference of $\overline{\theta_{p-}}$ and $\overline{\theta_{p+}}$ tend to decrease, and following approximation is materialized.

$$\overline{\theta_{p+}} \simeq \overline{\theta_{p-}} \tag{8}$$

Cumulative distributions of the ratio of $\overline{\theta_{p-}}$ and $(\theta_{p-\max} - \theta_V)$, the ratio of $\overline{\theta_{p+}}$ and $(\theta_{p+\max} + \theta_V)$ are shown in Figure 7(b), (c), respectively. As shown in Figure 7(b), (c), the ratio of $\overline{\theta_{p+}}$ and $(\theta_{p+\max} + \theta_V)$ has large variation compared with the ratio of $\overline{\theta_{p-}}$ and $(\theta_{p-\max} - \theta_V)$ in such a small range that $(\theta_{p+\max} + \theta_V)$ ranges between 0.005 and 0.01. This ratio is distributed uniformly between 0.5 and 2. However, as a plastic defor-

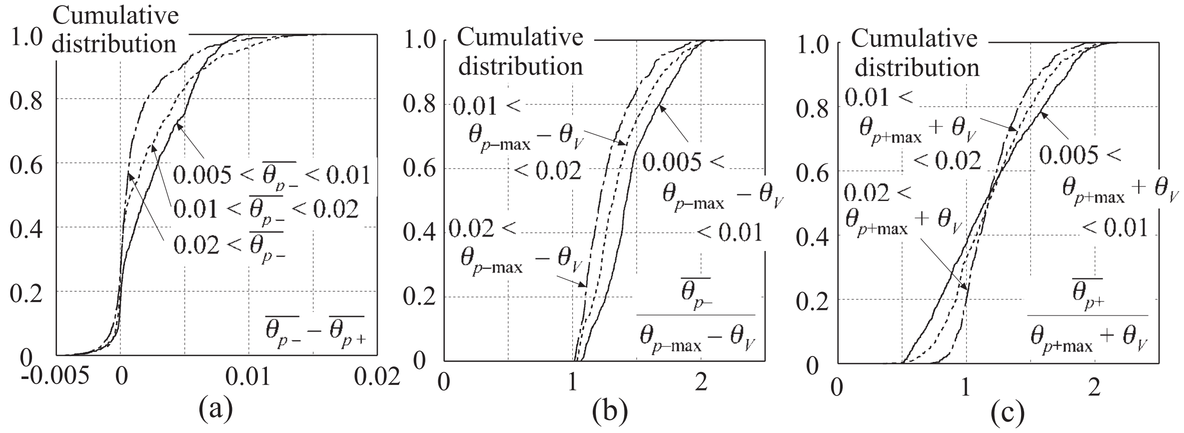

Figure 7: (a) $\overline{\theta_{p-}} - \theta_{p+}$ (b) $\overline{\theta_{p-}} / (\theta_{p-\max} - \theta_V)$ (Negative bending), (c) $\overline{\theta_{p+}} / (\theta_{p+\max} + \theta_V)$ (Positive bending).

mation become large, it is recognized that these ratios tend to concentrate between 1 and 1.5.

$$\theta_{p-\max} - \theta_V < \overline{\theta_p} < 1.5\,(\theta_{p-\max} - \theta_V) \tag{9}$$

4. CONCLUSION

In this paper, an evaluation of maximum numerical results of plastic deformation introduced into beam-ends on the basis of earthquake response analysis for 15 steel moment-resistant frames was discussed. The results are summarized as follows.

(1) The largest values in each story of plastic rotation at beam-ends ($\theta_{p\,\max}$) were occurred by negative bending that upper flanges are subjected to tension force, and can be approximated as follows.

$$\theta_{p\,\max} \simeq \theta_{p-\max} \simeq \min\left\{\frac{3}{2}\,(R_{\max} - R_y)\,,\, R_{\max}\right\} \tag{10}$$

In which R_y is the story drift angles when plastic hinges were first formed at beam-ends.

(2) Maximum plastic rotation of positive bending at beam-ends ($\theta_{p+\max}$) could be approximated by using maximum plastic rotation of negative bending in each story ($\theta_{p-\max}$).

$$\theta_{p+\max} \simeq \theta_{p-\max} - 2\theta_V \tag{11}$$

In which θ_V is the rotation of a simple beam under static vertical loading.

(3) Maximum increment of plastic rotation during a half-cycle of vibration ($\Delta\,\theta_{p\,\max}$) was approximately equal to maximum plastic rotation at beam-ends.

$$\Delta\theta_{p\,\max} \simeq \theta_{p-\max} \tag{12}$$

(4) The range of variable plastic rotation ($\overline{\theta_p}$) ranged from 1 to 1.5 of ($\theta_{p-\max} - \theta_V$) .

$$\theta_{p-\max} - \theta_V < \overline{\theta_p} < 1.5\,(\theta_{p-\max} - \theta_V) \tag{13}$$

References

[1] Takashi Hasegawa, et al. (1998). Comparison between seismic performance of U.S. steel perimeter and Japanese spatial moment resisting frames (Part1 Model buildings and structural performance). Summaries of Technical Papers of Annual Meeting Architectural Institute of Japan, 903-904 (in Japanese).

[2] Susumu Kuwahara, et al. (1998). Strength Ratio and An Approximate Calculation for The Plastic Collapse Load Considering Joint Panels. Journal of Constructional Steel. 6, 357-362 (in Japanese).

[3] P. Somerville, et al. (1997). Development of Ground Motion Time Histories for Phase 2 of the FEMA/SAC steel Project. Report No. SAC/BD-97-04, SAC joint Venture, 555 University Ave., Sacramento, CA.

[4] Koji Ogawa, et al. (2000). Ductility Demanded of Members in Steel Moment Frames Sustaining Beam-Hinging Mechanism. Journal of Structural and Construction Engineering. 537, 121-128 (in Japanese).